International Council for the Exploration of the Sea



ICES C.M. 1992/E:23
Marine Environmental Quality Committee

# Local Atmospheric Input Patterns in the German Bight

**Heinke Schlünzen, Klaus Bigalke, Ulrike Niemeier**

Meteorologisches Institut, Universität Hamburg,
Bundesstraße 55, D-2000 Hamburg 13

August 7, 1992

## Abstract

Examples are given for atmospheric input patterns in the area of the German Bight in a high temporal and spatial resolution. Total $NO_x$ and $SO_2$ input are calculated for a diurnal cycle by use of a three-dimensional atmospheric mesoscale model. Chemical transformation and wet deposition processes have been neglected for simplification. The modeled meteorological situations are representative for some typical weather conditions in spring, when the growth rate of the phytoplankton is at its maximum and the incoming short wave radiation is only minimally reduced by clouds.

The model results show that the calculated input does not always linearly decrease from the coastline. The main input is close to the coastline but there are local maxima also further from the coast over the water. They are caused by emittant distribution, as well as diurnal variations in the wind field, in the dry deposition over land and water, and in the efficiency of vertical exchange processes.

## 1 Introduction

Atmospheric input can make up more than half of the total input of contaminants into the ocean (e.g. Sündermann, 1992). Therefore, knowledge of the input amounts as well as of local atmospheric input patterns is essential for studies of tracer transport in water and tracer uptake by suspended matter and plankton. For studies of local phenomena in the ocean or of the ecosystem, the temporal resolution of the input values should be a few hours at most, the spatial resolution a few kilometers.

Up to now, most of the available input data consist of temporal and regional means. They are often based on results from long-range transport models which can be used for the estimation of the atmospheric input in time intervals of months and for regions of a few 10000 $km^2$ (see e.g. Schlünzen and Krell, 1992). Local input values cannot be derived from long-range transport models but comparatively easily from measurements due to their local nature. However, it is difficult to extend the validity of the measured values over other areas and over water. Results from mesoscale models can be used to close the gap between mean and local atmospheric input data. With these models the local input patterns can be calculated with a sufficient temporal (few minutes) and spatial (few kilometers) resolution.

In the three-dimensional mesoscale transport and fluid model METRAS used for the present local atmospheric input studies, wind, temperature, humidity and tracer concentrations ($SO_2$ and $NO_x$) are calculated from prognostic equations. The horizontal resolution of the model lies between $2.5km$ and $10km$, the time step is about one minute. The atmospheric input data (only dry deposition processes) are integrated to obtain hourly and daily figures. The dry deposition of the tracers is modeled following the resistance model concept. It depends on tracer concentration, atmospheric stability and type of tracer. For example, the $SO_2$ and $NO_x$ dry deposition values are different over water due to the different solubility of the two gases in water.

The influences of clouds, gravity waves, topographically induced effects, land- seabreezes and other mesoscale phenomena can be directly simulated in the model and do not have to be parameterized. All subgrid-scale turbulent processes are parameterized utilizing a first order closure hypothesis. The planetary boundary layer is vertically resolved. For details on the model see Schlünzen (1990) and Schlünzen and Pahl (1992).

# 2 Model Area and Initialization

The model area under investigation consists of the German Bight and the surrounding mainland (see Figure 1, left). The model grid is non-uniform in vertical as well as in horizontal directions. The lowest horizontal grid-size of $2.5km$ is placed in the estuary of the River Elbe to ensure a good representation of the North and East Friesian coastline and the Wadden Sea in the model. Towards the lateral boundaries the grid-size increases to $10km$ (Figure 1, right).

In the present paper, results of four model simulations are presented, one of them in detail. They correspond to typical weather conditions in spring. Offshore large-scale winds of $8.5ms^{-1}$ are prescribed. In particular results for large-scale winds from the east are given. The corresponding wind velocity and wind direction at a height of 10 m at Bremen are $4.15ms^{-1}$ and NE (north-east) winds. The 20 year mean frequency distribution of wind direction and velocity in May shows for Bremen a mean of $4.3ms^{-1}$ with values of $4.0ms^{-1}$, $5.4ms^{-1}$, and $3.6ms^{-1}$ at 700 LST, 1400 LST, and 2100 LST, respectively. The mean wind values are calculated by Bätjer and Heinemann (1983) from measurements.

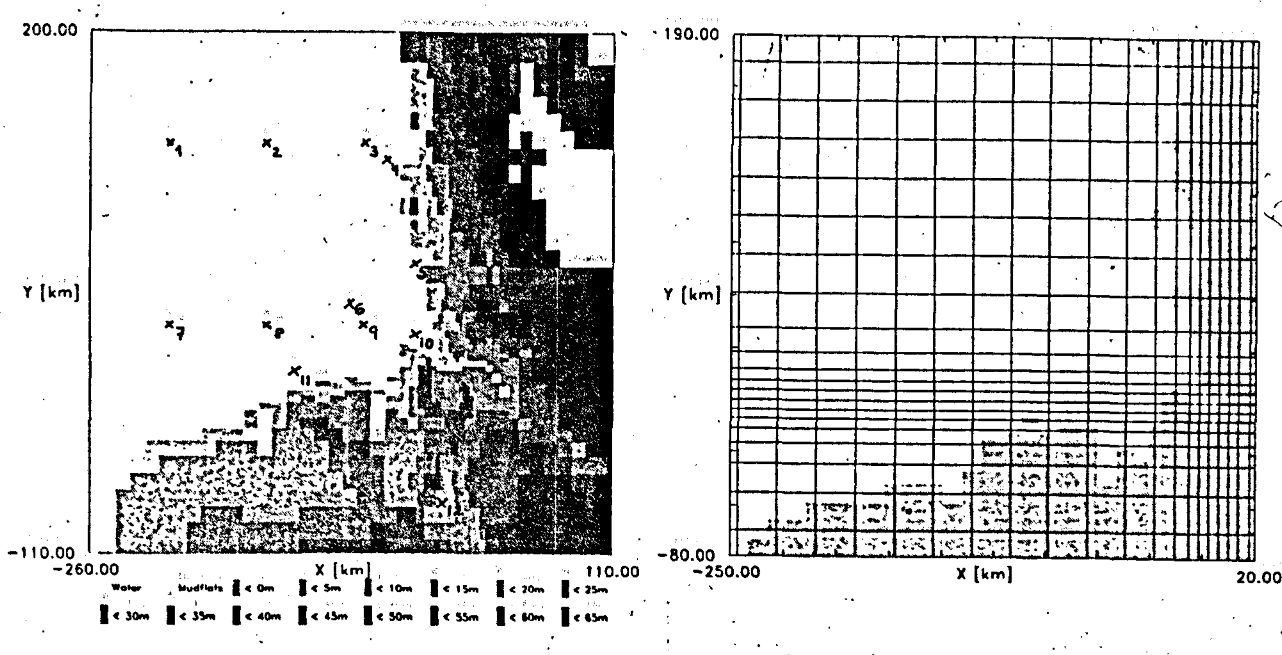


Figure 1: Topography in the full model area (left) and grid structure in part of the model area (right). The crosses refer to the sites used in Table 2 for the calculation of daily input values.

From the frequency distribution in Table 1 it can clearly be seen that wind velocities between 3.4 and 5.4 $ms^{-1}$ are most frequent, they comprise 34.3% of all situations. The frequency distribution shows no strong dependence of the wind velocity on the wind direction, only southerly winds occur quite seldom.

| Wind Velocity | Wind Direction | | | | | | | | Sum |
|---|---|---|---|---|---|---|---|---|---|
| $[ms^{-1}]$ | N | NE | E | SE | S | SW | W | NW | |
| 0.1 - 1.5 | 0.9 | 1.3 | 1.3 | 1.3 | 1.2 | 1.6 | 1.6 | 1.4 | 10.6 |
| 1.6 - 3.3 | 2.8 | 3.5 | 3.9 | 4.1 | 2.6 | 3.6 | 3.7 | 4.8 | 29.0 |
| 3.4 - 5.4 | 3.9 | 4.0 | 5.5 | 3.3 | 2.0 | 4.0 | 5.5 | 6.1 | 34.3 |
| 5.5 - 7.9 | 1.6 | 1.2 | 2.8 | 1.5 | 1.1 | 3.1 | 4.1 | 4.5 | 19.9 |
| 8.0 - 10.7 | 0.3 | 0.1 | 0.5 | 0.4 | 0.2 | 1.0 | 1.7 | 1.3 | 5.5 |
| 10.8 - 17.1 | - | - | - | - | - | 0.3 | 0.2 | 0.2 | 0.7 |
| Sum | 9.5 | 10.1 | 14.0 | 10.6 | 7.1 | 13.6 | 16.8 | 18.3 | 100 |

Table1: Frequency [%] of wind velocities for a 20 year mean May dependent on wind directions at a height of $10m$ at Bremen. The values are derived from Table 159 in Bätjer and Heinemann (1983).

Meteorological situations with NE, E, SE or S winds at Bremen have been taken into account for the calculation of local input patterns. The wind directions correspond to offshore winds close to the surface and to large-scale winds from east, southeast, south or southwest. Other wind directions have been neglected, since only very few input into the German Bight can be expected for them in view of the emittant distribution. In the model calculations, the emittants in the Federal Republic of Germany are included, whereas emittants in Denmark or the Netherlands are neglected (see Figure 2). Emittants outside the model area are not explicitly taken into account; zero tracer flux through the boundaries is assumed.

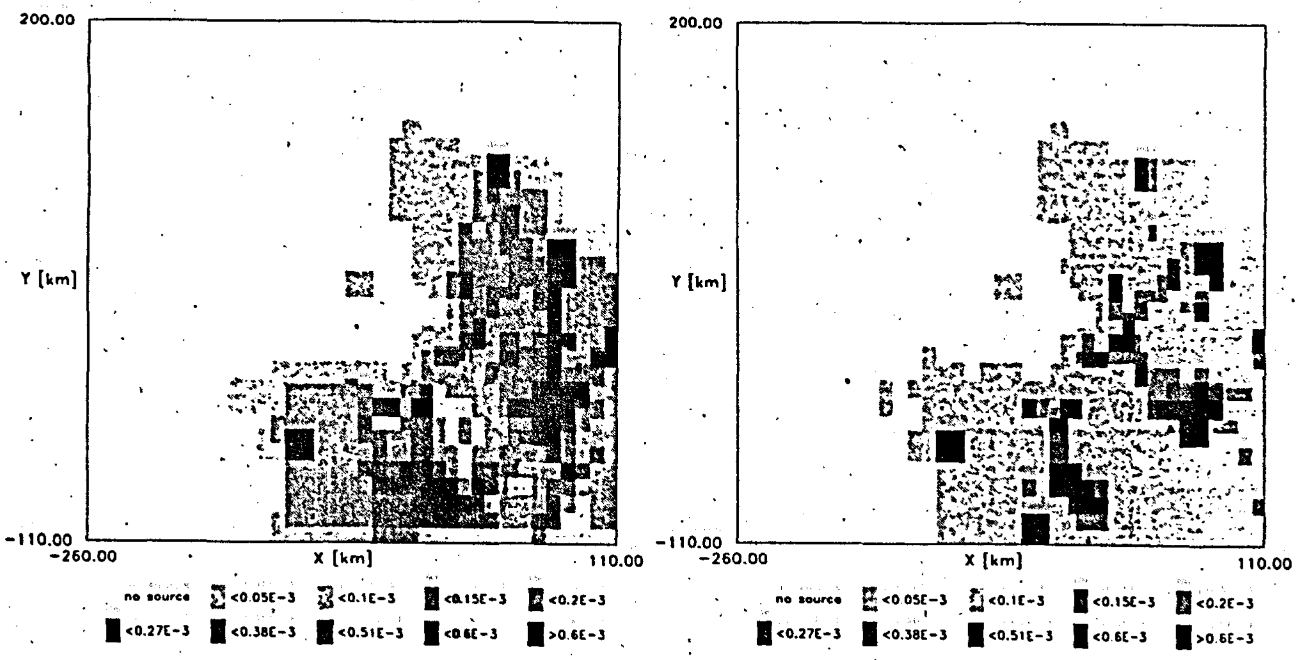


Figure 2: Total $NO_x$ (left) and $SO_2$ (right) emittants (data base: UBA, 1989).

Large-scale atmospheric stability is prescribed from mean values for May derived from data of the "Europäischer Wetterbericht" (Deutscher Wetterdienst) for the years 1982 to 1989. The stratification is strongly stable close to the ground ($0.67K(100m)^{-1}$ up to $600m$), slightly stable above ($0.37K(100m)^{-1}$ up to an altitude of $1000m$) and in larger altitudes ($0.41K(100m)^{-1}$). The surface temperature is 12 ° C at the beginning of the model run and changes dependent on the atmospheric radiation budget. The water temperature at the surface is kept at a constant of 9 ° C for the whole model run.

Balanced wind-, temperature-, and humidity-profiles are calculated from the large-scale wind and stratification with a one-dimensional version of the model. These are used as input values for the three-dimensional model in which the topography is introduced via diastrophism. Since the tracer concentration is zero within the whole model area at the begining of the model run, an initialization time period of 21 hours is necessary to calculate the starting tracer concentration fields (see Figure 3). The initialization period runs from midnight of the initialization day to 2100 LST of that day. The model calculations are performed for a further 24 hours (one diurnal cycle), starting at 2100

LST with the integration of the diurnal input values.

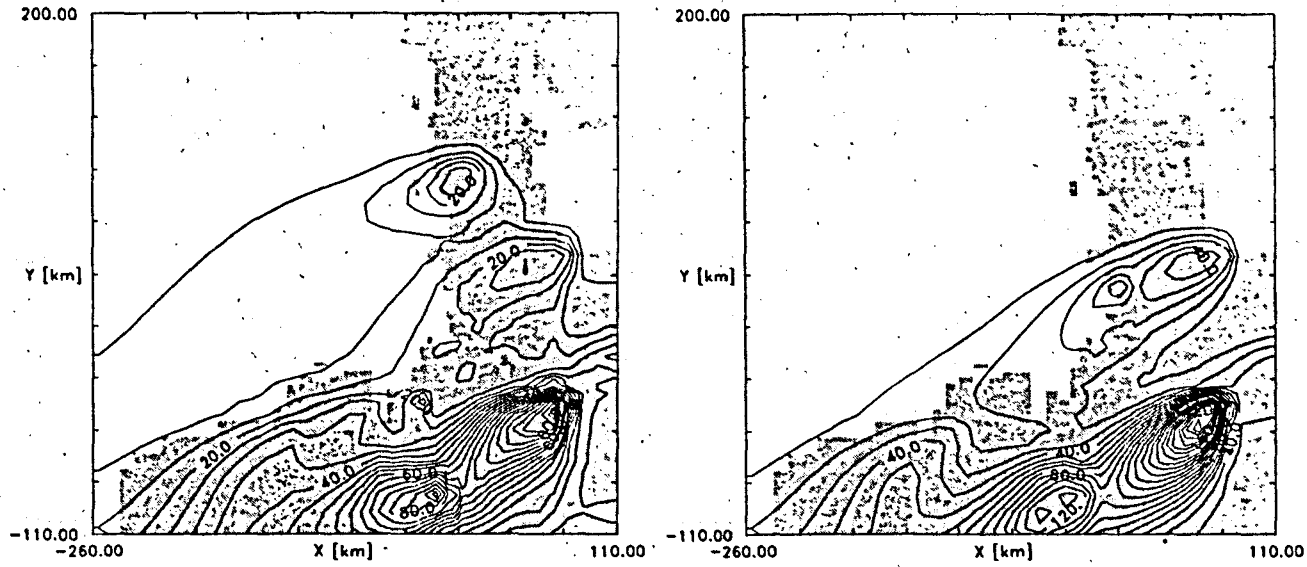


Figure 3: Starting tracer concentration fields of $NO_x$ (left, increment $5[\mu g\, kg^{-1}]$) and $SO_2$ (right, increment $10[\mu g\, kg^{-1}]$) at a height of $10m$ above ground for a large-scale east wind at 2100 LST (initialization day).

# 3 Local Input Patterns for Large-Scale East Wind

A large-scale east wind corresponds to E-NE winds at a height of $10m$ (Figure 4, top). During the day, the changes in the wind direction are quite small and lie in a range of $10^\circ$ only. The changes in the wind velocities are larger. They are between $2.4ms^{-1}$ and $8.1ms^{-1}$ at 600 LST (Figure 4, left) and increase over land ($3.0ms^{-1}$ to $8.1ms^{-1}$ at 1500 LST, Figure 4, right) during the day. They are reduced again over land in the evening and during night. In the area of the German Bight the wind velocities remain about the same; a diurnal cycle cannot be found here.

The processes which are important for transport, namely the atmospheric advection and exchange processes, have to be examined to understand the input patterns. It could be expected that more tracers are transported to the sea in the afternoon when the wind velocities are higher. At this time the advection is stronger but the tracer concentration is lower. Because of the surface heating over land an unstable stratification develops there at daytime and the $NO_x$ and $SO_2$ are mixed up to higher layers of the atmosphere. This reduces the concentration in lower layers during the day to a minimum in the afternoon. The concentration becomes gradually higher during nighttime. Over land and the coastal water the concentration in air reaches maximum values in the early morning.

The outlined diurnal cycle of the concentration field over the German Bight characterizes the hourly input values, if wet deposition is neglected. This can be seen in the

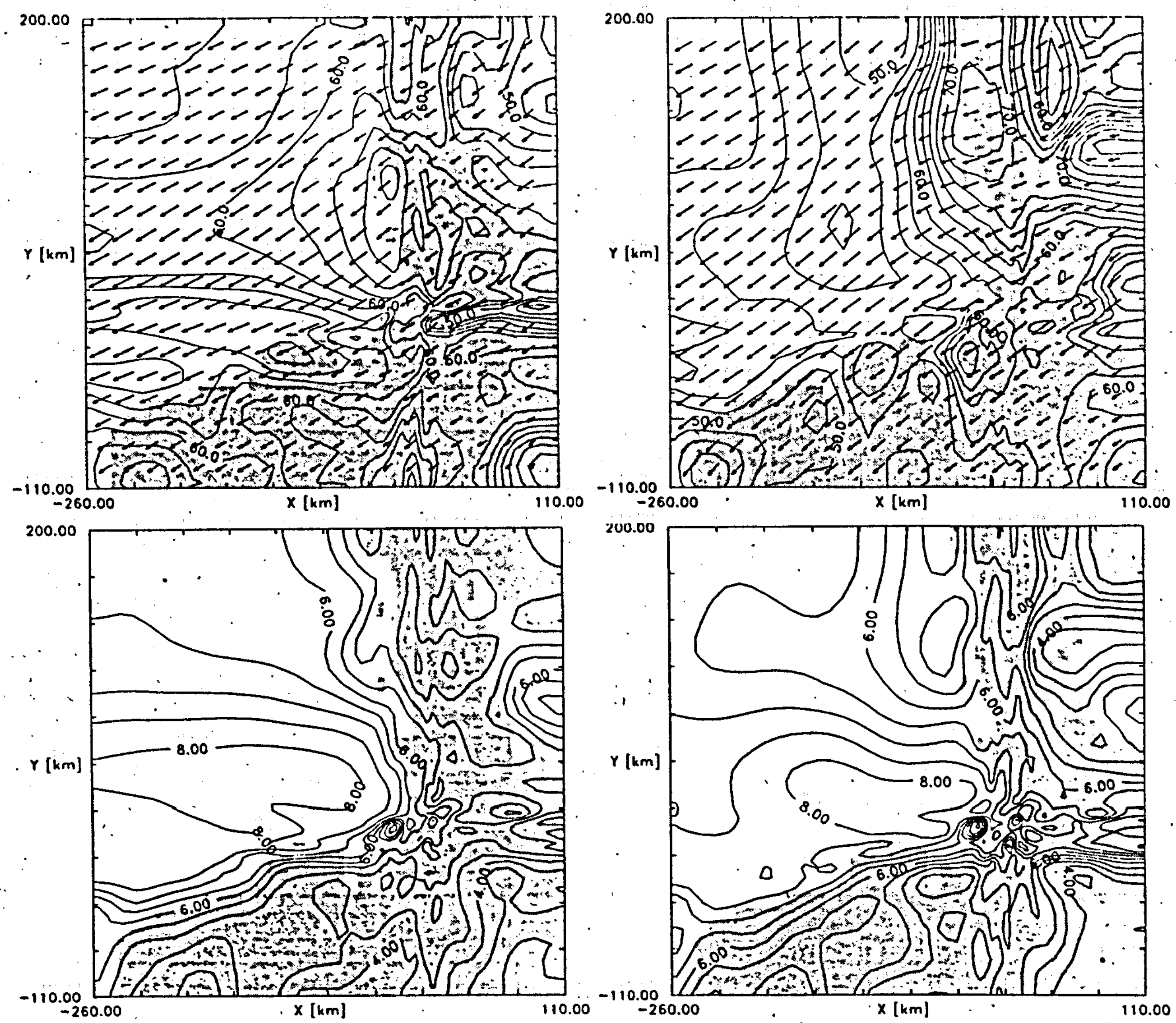


Figure 4: Wind direction (top, increment 2.5[°]) and wind velocity (bottom, increment $0.5[ms^{-1}]$) at 600 LST (left) and at 1500 LST (right) at a height of $10m$ above ground, increment 2.5[°].

model results. The concentration fields have maxima over water in the morning and minima in the late evening (figures not shown here). These are reflected by the calculated input values for $NO_x$. They result in higher input numbers in the morning (e.g. at Helgoland $0.08[mg\,m^{-2}h^{-1}]$ at 600 LST, Figure 5, top left) and reduced input in the evening ($0.05[mg\,m^{-2}h^{-1}]$ at 2100 LST, Figure 5, bottom right). During daytime the input continuously decreases. The diurnal differences in the dry deposition are lower over water compared to the changes over land. Here a diurnal cycle in the deposition velocity characterizes the dry deposition. The deposition velocity is reduced at nighttime by a factor of six compared to daytime values. Over water the values remain about the same.

The diurnal cycle presented for $NO_x$ (Figure 5) is also found for $SO_2$ (Figure 6). Differences in the input patterns of the two tracers are mainly explained by differences in

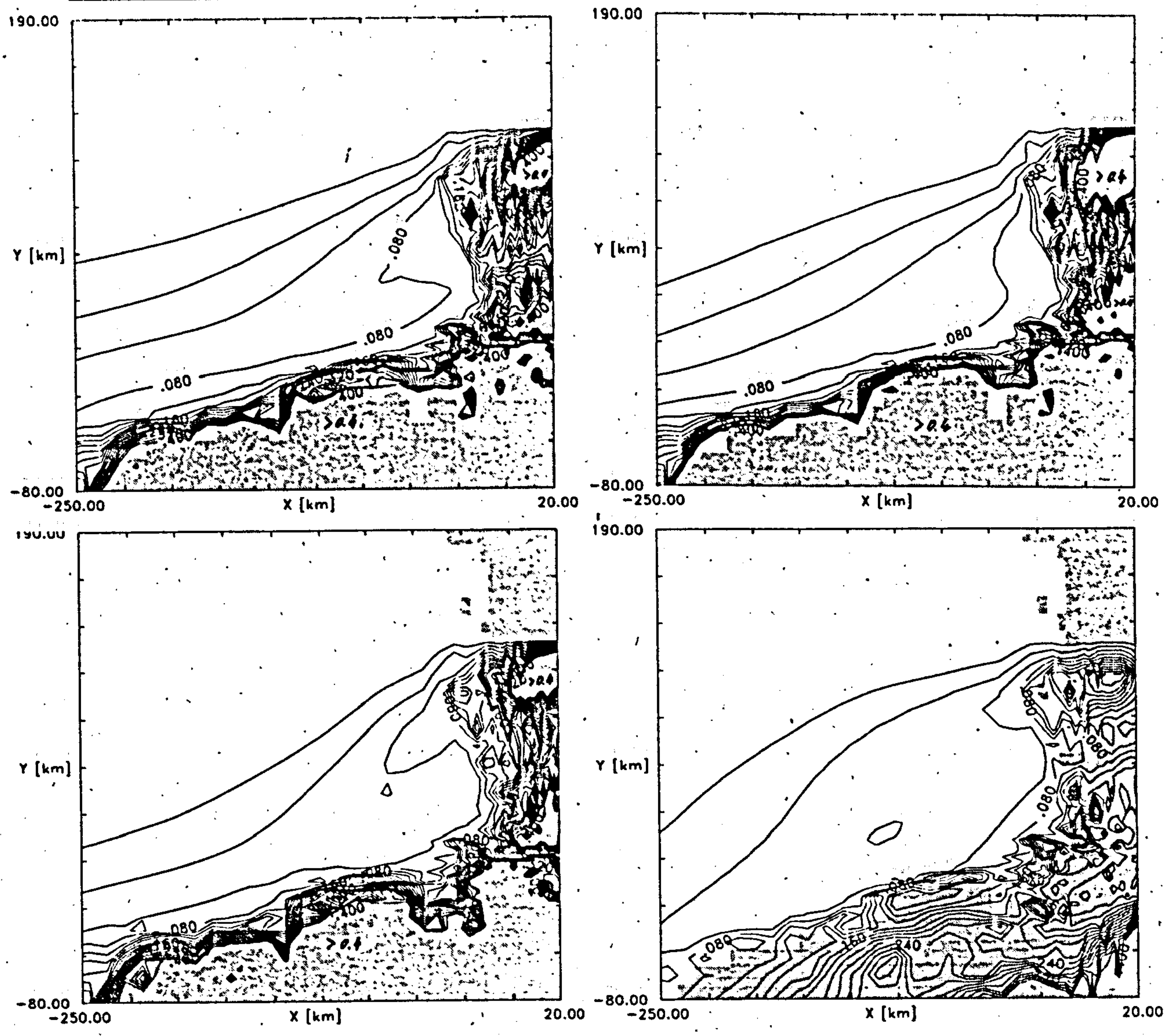


Figure 5: Hourly dry deposited $NO_x$ for a large-scale east wind in part of the model area at 600 LST, 900 LST, 1500 LST, 2100 LST, increment $0.02[mg\,m^{-2}h^{-1}]$.

the emittant distributions. In general, the input is higher for $SO_2$ because the emission rate is higher and the tracer has a better solubility in water than $NO_x$. The maximum for the hourly dry deposition cannot be found at 600 LST but at 2100 LST in the Elbe estuary. This maximum is caused by a locally higher concentration of $SO_2$ in this area in the evening. Due to a slightly different wind direction (64° at 600 LST, 56° at 2100 LST), emittet tracers from sources in the area of Husum are transported further north over the sea. This causes locally higher concentrations and thus locally higher input values at 2100 LST compared to 600 LST.

The calculated hourly input caused by dry deposition is integrated over 24 hours to get input values characteristic for the day. These input patterns show a strong decrease towards the open sea (Figure 7). In reality, the gradient might be reduced since emitted tracers from Denmark would be advected into the northern part of the model area. The input is very high in the Wadden Sea area, especially for $SO_2$. The maximum in the

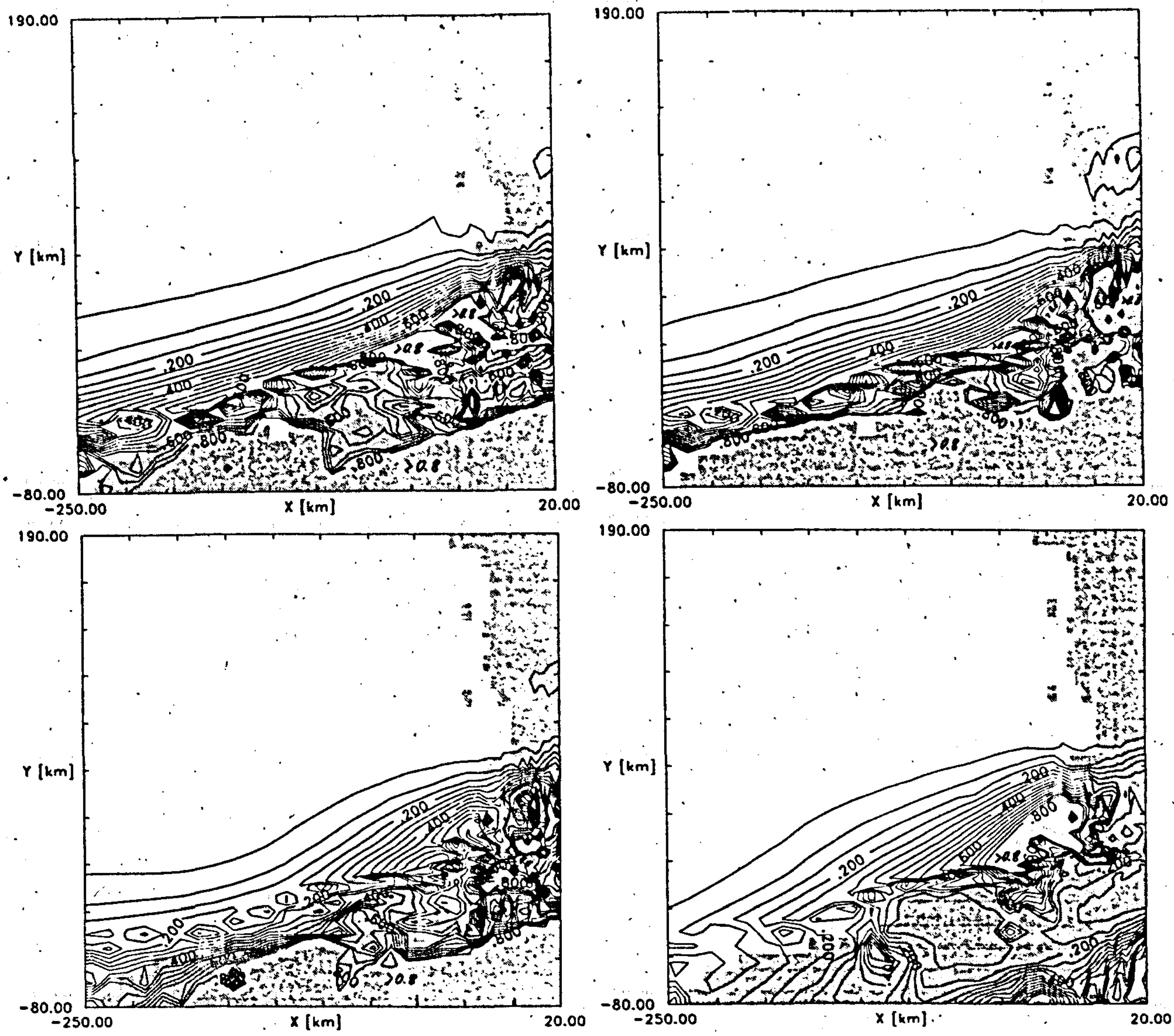


Figure 6: Hourly dry deposited $SO_2$ for a large-scale east wind in part of the model area at 600 LST, 900 LST, 1500 LST, 2100 LST, increment $0.05[mg\,m^{-2}h^{-1}]$.

southeast part of the German Bight is caused by emissions in the Elbe estuary by ships using sulphurous fuel. The input into that area as well as into the whole German Bight will be higher if the emissions from ships traveling there are included in the model calculations.

# 4 Assessment of the Model Results

In this paper detailed results are given for a case study which is representative for typical meteorological conditions in spring. Results for large-scale southeast, south or southwest winds show similar diurnal cycles but differences in the actual structures. In Figure 8 the integrated dry deposition is presented for a meteorological situation with a large-scale wind from southwest. It can be seen that the input into the water in the

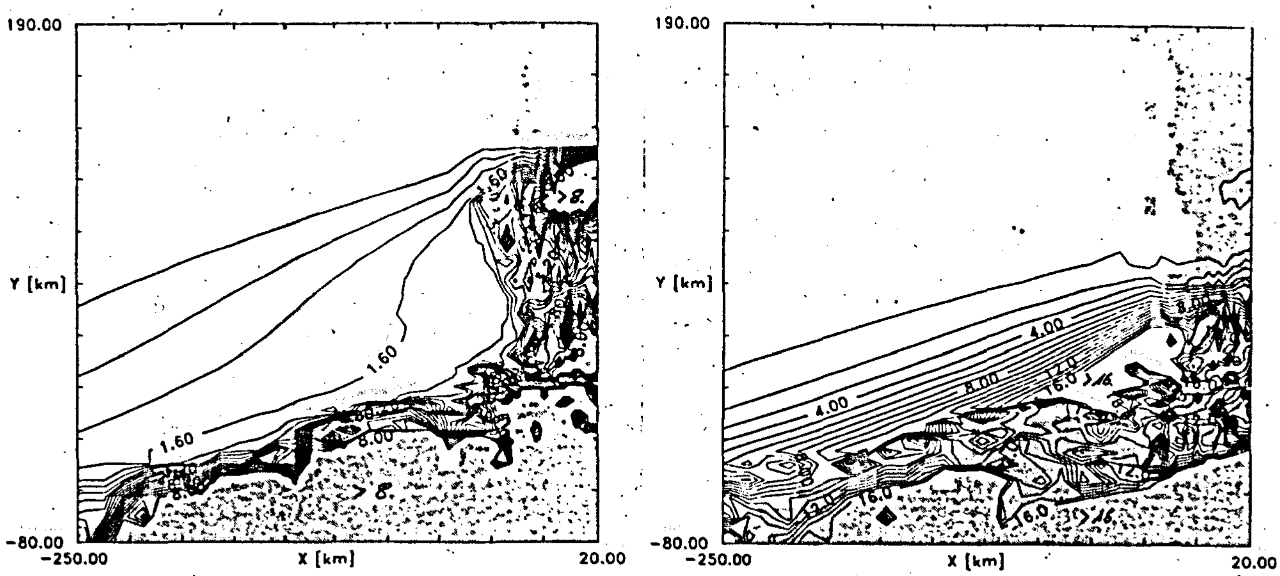


Figure 7: Dry deposited $NO_x$ (left, increment $0.4[mg\,m^{-2}d^{-1}]$) and $SO_2$ (right, increment $1.0[mg\,m^{-2}d^{-1}]$) integrated for 24 hours for a large-scale east wind in part of the model area.

area of the Elbe estuary is lower for both tracers compared to the case calculated with a large-scale east wind (Figure 7). In contrast, in the western model area the atmospheric input is higher for a large-scale southwest wind. Here, emissions from coastal emittants in the area of Emden increase the concentration of tracers in air and thus cause higher inputs. They might be even higher if emittants in the Netherlands are included in the model calculations.

The model results of the four case studies are compiled in Table 2 for some selected sites in the model area. In general, the input of $SO_2$ is higher compared to that of $NO_x$. This is partly a result of differences in the emittant characteristics (Figure 2) but mainly caused by the good solubility of $SO_2$ in water. The highest input values are calculated in the present case studies for a large-scale southeast wind when high tracer concentrations caused by emissions in the populated areas are transported towards the German Bight. In this case the input is enlarged by a factor of 2 to 10 compared to other wind directions.

Areas with high emission rates are closest to the sea for the calculated offshore wind directions. Thus, the proportion to the total input into the German Bight might be highest. For other large-scale wind directions the proportion into the German Bight is in general quite low (Kriews, 1992) and has been neglected when calculating the integrated daily input values for Table 2. The weighted mean input data show again the higher numbers for the $SO_2$ input. For this tracer not only maxima at the coastline but further offshore (54 ° N 7 ° E) can be found. The $NO_x$ input data do not show local maxima further offshore but have maxima in the Wadden Sea area.

The presented numbers characterize the lower limit of the input data. However, the numbers might be reduced further if wet deposition processes or chemical transforma-

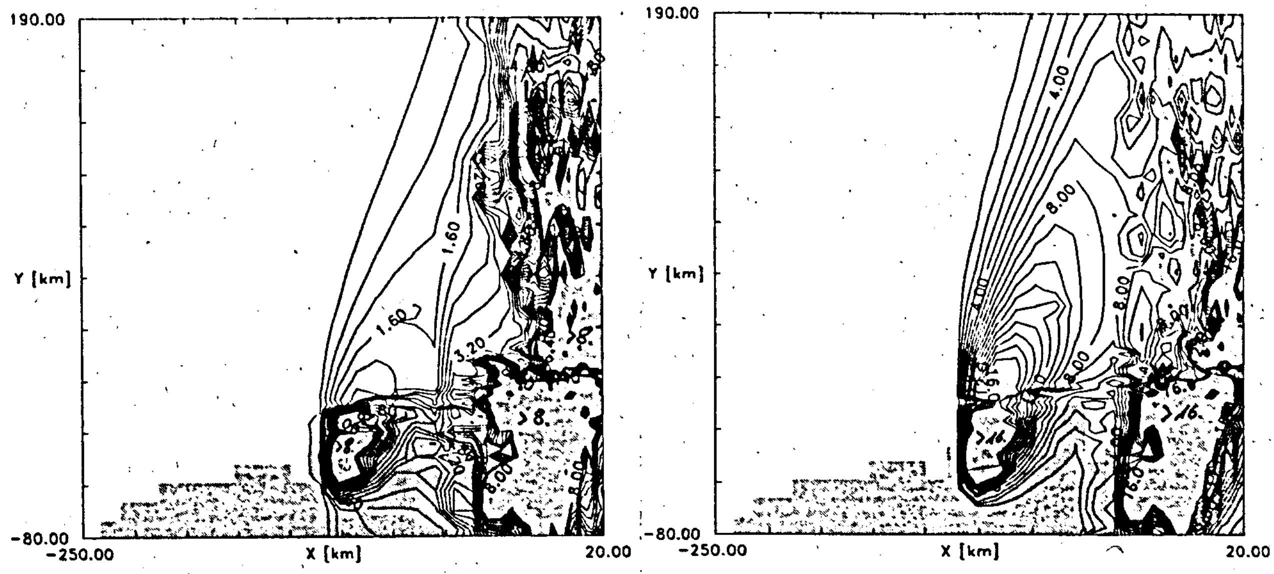


Figure 8: Dry deposited $NO_x$ (left, increment $0.4[mg\,m^{-2}d^{-1}]$) and $SO_2$ (right, increment $1.0[mg\,m^{-2}d^{-1}]$) integrated for 24 hours for a large-scale southwest wind in part of the model area.

tion would be included in the model calculations. In any case, the consideration of emission data from Denmark and the Netherlands and of tracer fluxes through the lateral boundaries will result in higher input values. To get more complete input statistics, additional case studies (other wind velocities for May, other months, inclusion of wet deposition processes, inclusion of chemical transformation, inclusion of emission data from Denmark and the Netherlands, inclusion of fluxes via lateral boundaries) have to be performed.

| | Site | Large-Scale Wind Direction NE | E | SE | S | SW | W | NW | N | Weighted Mean |
|---|---|---|---|---|---|---|---|---|---|---|
| F[%] | 12: Bremen | 9.5 | 10.1 | 14.0 | 10.6 | 7.1 | 13.6 | 16.8 | 18.3 | 100.0 |
| $NO_x$ | 1: 55°N 6°E | 0[1] | 0[2] | 7.0 | 0[3] | 0[3] | 0[1] | 0[1] | 0[1] | 1.0[4] |
| $NO_x$ | 2: 55°N 7°E | 0[1] | 0[2] | 7.0 | 4.0 | 0[3] | 0[1] | 0[1] | 0[1] | 1.4[4] |
| $NO_x$ | 3: 55°N 8°E | 0[1] | 0[2] | 6.0 | 4.8 | 1[3] | 0[1] | 0[1] | 0[1] | 1.4[4] |
| $NO_x$ | 4: Westerland | 0[1] | 0[2] | 8.0 | 6.0 | 1.6 | 0[1] | 0[1] | 0[1] | 1.9[4] |
| $NO_x$ | 5: Westerhever | 0[1] | 2.5 | 15.0 | 6.0 | 4.0 | 0[1] | 0[1] | 0[1] | 3.3[4] |
| $NO_x$ | 6: Helgoland | 0[1] | 1.7 | 9.0 | 6.0 | 1.6 | 0[1] | 0[1] | 0[1] | 2.2[4] |
| $NO_x$ | 7: 54°N 6°E | 0[1] | 1[2] | 7.9 | 0[3] | 0[3] | 0[1] | 0[1] | 0[1] | 1.2[4] |
| $NO_x$ | 8: 54°N 7°E | 0[1] | 1.4 | 7.9 | 3[3] | 0[3] | 0[1] | 0[1] | 0[1] | 1.6[4] |
| $NO_x$ | 9: 54°N 8°E | 0[1] | 1.8 | 8.5 | 6.0 | 2.0 | 0[1] | 0[1] | 0[1] | 2.2[4] |
| $NO_x$ | 10: Elbe Esturay | 0[1] | 2.5 | 8.5 | 5.0 | 3.6 | 0[1] | 0[1] | 0[1] | 2.2[4] |
| $NO_x$ | 11: Norderney | 0[1] | 2.0 | 9.5 | 3[3] | 2[3] | 0[1] | 0[1] | 0[1] | 2.0[4] |
| $SO_2$ | 1: 55°N 6°E | 0[1] | 0[2] | 34.0 | 7[3] | 0[3] | 0[1] | 0[1] | 0[1] | 5.5[4] |
| $SO_2$ | 2: 55°N 7°E | 0[1] | 0[2] | 32.0 | 14.5 | 0[3] | 0[1] | 0[1] | 0[1] | 6.0[4] |
| $SO_2$ | 3: 55°N 8°E | 0[1] | 0[2] | 26.0 | 17.5 | 6[3] | 0[1] | 0[1] | 0[1] | 5.9[4] |
| $SO_2$ | 4: Westerland | 0[1] | 0[2] | 24.0 | 20.0 | 6.0 | 0[1] | 0[1] | 0[1] | 5.9[4] |
| $SO_2$ | 5: Westerhever | 0[1] | 1.8 | 45.0 | 20.0 | 8.0 | 0[1] | 0[1] | 0[1] | 9.2[4] |
| $SO_2$ | 6: Helgoland | 0[1] | 3.0 | 54.0 | 24.0 | 12.0 | 0[1] | 0[1] | 0[1] | 11.3[4] |
| $SO_2$ | 7: 54°N 6°E | 0[1] | 1[2] | 40.0 | 2[3] | 0[3] | 0[1] | 0[1] | 0[1] | 5.9[4] |
| $SO_2$ | 8: 54°N 7°E | 0[1] | 3.5 | 47.0 | 11[3] | 0[3] | 0[1] | 0[1] | 0[1] | 8.1[4] |
| $SO_2$ | 9: 54°N 8°E | 0[1] | 13.5 | 47.0 | 24.0 | 9.0 | 0[1] | 0[1] | 0[1] | 11.1[4] |
| $SO_2$ | 10: Elbe Esturay | 0[1] | 24.0 | 38.0 | 6.0 | 10.0 | 0[1] | 0[1] | 0[1] | 9.1[4] |
| $SO_2$ | 11: Norderney | 0[1] | 13.0 | 40.0 | 13[3] | 16[3] | 0[1] | 0[1] | 0[1] | 9.4[4] |

Table2: Frequency F[%] of large-scale wind directions derived from wind measurements at Bremen for a 20 year mean May (see Table 1) and calculated daily input values [$mg\,m^{-2}d^{-1}$] at specified sites. For the location of the sites see numbers in Figure 1.

[1]Input not calculated for this case but assumed to be zero.

[2]Input values presumably too low due to missing emissions from Denmark

[3]Input values presumably too low due to missing emissions from the Netherlands

[4]The weighted input values are presumably too low due to missing emissions from Denmark and the Netherlands

# Acknowledgements

This work was funded by the "Bundesminister für Forschung und Technologie" under grant numbers MFU 0620/6 and 03 F0037A, and by the Universität Hamburg.


# 5 References


Bätjer,D. and Heinemann,H.-J. (1983): Das Klima ausgewählter Orte der Bundesrepublik Deutschland - Bremen. Selbstverlag des Deutschen Wetterdienstes, Offenbach am Main, pp251.

Kriews,M. (1992): Charakterisierung mariner Aerosole in der Deutschen Bucht sowie Prozeßstudien zum Verhalten von Spurenmetallen beim Übergang Atmosphäre/Meerwasser. Dissertation, Fachbereich Chemie, Universität Hamburg

Schlünzen,K.H. (1990): Numerical studies on the inland penetration of sea-breeze fronts at a coastline with tidally flooded mudflats. Beitr. Physik Atmos., 63, 243-256

Schlünzen,K.H. and Krell,U. (1992): Mean and local transport in air. in: "Circulation and contaminant fluxes in the North Sea", ed. J. Sündermann, Springer Verlag, Heidelberg (in preparation)

Schlünzen,K.H. and Pahl,S. (1992): Modification of dry deposition in a developing sea-breeze circulation - a numerical case study. Atmosph. Envir., 26A, 51-61

Sündermann,J. (1992): Circulation and contaminant fluxes in the North Sea. Springer Verlag, Heidelberg (in preparation)

UBA (1989): Daten zur Umwelt 1988/89. Erich Schmidt Verlag, Berlin.